

GraphDLG: Exploring Deep Leakage from Gradients in Federated Graph Learning

Shuyue Wei*

C-FAIR & School of Software
Shandong University
Jinan, China
weishuyue@sdu.edu.cn

Chen Gong

Automation & Intelligent Sensing
Shanghai Jiao Tong University
Shanghai, China
chen.gong@sjtu.edu.cn

Wantong Chen*

SKLCCSE Lab
Beihang University
Beijing, China
2306cwt@buaa.edu.cn

Tongyu Wei

SKLCCSE Lab
Beihang University
Beijing, China
weitongyu@buaa.edu.cn

Yongxin Tong

SKLCCSE Lab
Beihang University
Beijing, China
yxtong@buaa.edu.cn

Lizhen Cui

C-FAIR & School of Software
Shandong University
Jinan, China
clz@sdu.edu.cn

ABSTRACT

Federated graph learning (FGL) has recently emerged as a promising privacy-preserving paradigm that enables distributed graph learning across multiple data owners. A critical privacy concern in federated learning is whether an adversary can recover raw data from shared gradients, a vulnerability known as deep leakage from gradients (DLG). However, most prior studies on the DLG problem focused on image or text data, and it remains an open question whether graphs can be effectively recovered, particularly when the graph structure and node features are uniquely entangled in GNNs.

In this work, we first theoretically analyze the components in FGL and derive a crucial insight, *i.e. once the graph structure is recovered, node features can be obtained through a closed-form recursive rule*. Building on our analysis, we propose GraphDLG, a novel approach to recover raw training graphs from shared gradients in FGL, which can utilize randomly generated graphs or client-side training graphs as the auxiliaries to enhance the recovery. Extensive experiments demonstrate that our GraphDLG outperforms existing solutions by successfully decoupling the graph structure and node features, achieving improvements of over 5.46% (by MSE) for node feature reconstruction and over 25.04% (by AUC) for graph structure reconstruction.

CCS CONCEPTS

• Computing methodologies → Learning paradigms.

KEYWORDS

Federated Graph Learning; Deep Leakage from Gradients

Permission to make digital or hard copies of all or part of this work for personal or classroom use is granted without fee provided that copies are not made or distributed for profit or commercial advantage and that copies bear this notice and the full citation on the first page. Copyrights for components of this work owned by others than the author(s) must be honored. Abstracting with credit is permitted. To copy otherwise, or republish, to post on servers or to redistribute to lists, requires prior specific permission and/or a fee. Request permissions from permissions@acm.org.

Conference acronym 'XX, June 03–05, 2018, Woodstock, NY

© 2026 Copyright held by the owner/author(s). Publication rights licensed to ACM.

ACM ISBN 978-1-4503-XXXX-X/18/06

<https://doi.org/XXXXXX.XXXXXXX>

ACM Reference Format:

Shuyue Wei*, Wantong Chen*, Tongyu Wei, Chen Gong, Yongxin Tong, and Lizhen Cui. 2026. GraphDLG: Exploring Deep Leakage from Gradients in Federated Graph Learning. In *Proceedings of Make sure to enter the correct conference title from your rights confirmation email (Conference acronym 'XX)*. ACM, New York, NY, USA, 13 pages. <https://doi.org/XXXXXX.XXXXXXX>

1 INTRODUCTION

Graphs naturally model the complex relationships or interactions among entities and serve as a prominent data for various real-world applications such as bioinformatics [23, 57], transportation [19, 43, 47], and healthcare [4, 5]. Notably, in many real scenarios, graph data is distributed across multiple data owners and it is prohibited to share the raw graphs directly due to strict data privacy regulations (e.g. GDPR [35] and CPRA [6]). For example, it is promising to train a graph learning model for drug discovery that utilizes extensive graph-based molecular data held by multiple individual drug research institutions. However, directly sharing the raw graphs among these institutions is usually infeasible due to privacy constraints. As a solution, federated graph learning (FGL) [9, 12, 26] has been emerging as a novel paradigm to tackle distributed graph data, which extends the concepts of federated learning [20, 42, 48] to graph data and enables the sharing of gradients in the learning process rather than raw graph data, thereby regarded as a privacy preserving way to protect the underlying graph information.

In federated learning, a problem known as *deep leakage from gradients (DLG)* has been identified as a fundamental privacy concern when sharing the gradients [53, 56, 59], *i.e. is it possible to recover private training data from the shared gradients during the federated learning process?* Prior works have studied the DLG problem across various data types and have empirically or theoretically demonstrated that raw training data, such as images [13, 58, 59], texts [7, 15], and tabular data [38], can be effectively recovered from the shared gradients in federated learning. Exploring the DLG issue on graph data is crucial for us to understanding the potential privacy risks in FGL. *Yet, it remains an unresolved question whether we can recover raw training graphs from shared gradients in FGL.* In this work, we aim to study the DLG problem inherent in FGL.

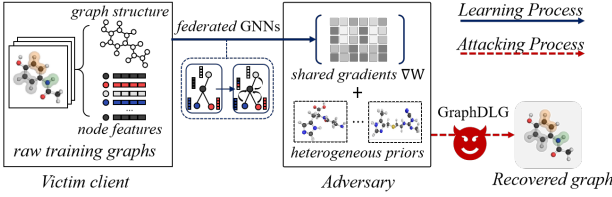


Figure 1: DLG for Graphs: In federated graph learning, an adversary can recover training graphs from the victim client’s gradients.

As shown in Fig. 1, the DLG for graphs in FGL poses unique challenges inherent to graph data and existing solutions for recovering training data from gradients face two significant limitations.

- *Limitation 1: Existing recovering approaches are not tailored for the graph neural network models (GNNs).* Unlike the targeted images or text, graphs consist of node features and unique topologies. It is common to adopt GNNs to tackle graph data, where the message aggregation operations intertwine node features and graph topologies within the gradients. Thus, prior solutions [7, 13, 15, 38, 59] for images or texts fail to disentangle node features and graph structures, making it ineffective to recover graphs (as in Tab. 5).

- *Limitation 2: Neglecting the heterogeneity between the prior knowledge and the target graphs to be recovered.* In existing studies [18, 25], the adversary is often assumed to leverage its local dataset as auxiliary priors to enhance recovery capability in DLG, as it is natural for an FL client to use its local training graphs as the auxiliary freely. However, prior solutions overlook the fact that an adversary’s auxiliary priors (e.g. local graphs) are usually heterogeneous with the victim client’s data to be recovered, a situation commonly encountered in real-world FGL scenarios [39, 49]. Thus, it is crucial to consider such heterogeneity between auxiliary and victim graphs when utilizing the auxiliary priors for DLG in FGL.

To address the above limitations in existing DLG attacks and better understand the associated privacy risk, we explore deep leakage from gradients in FGL and propose GraphDLG, which is graph-tailored and can effectively recover both the node features and graph structures of training graphs simultaneously. In this work, we focus on widely-used GCNs [21]. We first theoretically analyze the gradients of two essential components (MLP layers and GCN layers) in FGL and arrive at a crucial insight: *if the graph structure is known, node features can be recovered through a closed-form rule*, simplifying the graph-tailored DLG via decoupling node features and graph structures (in Sec. 4.1). Then, we design a decoder utilizing heterogeneous auxiliary priors to transform graph embeddings derived from the MLP layers in FGL into graph structures, thereby allowing publicly available or even randomly generated graphs to contribute to the graph-tailored DLG attacks (in Sec. 4.2). Finally, we substitute the obtained graph structures into our closed-form rules and recover node features of the target graph by recursively solving a set of linear equations (in Sec. 4.3). The main contributions and results are summarized as follows.

- We analyze gradients in FGL and derive a rule disentangling node features and graph structure, which provides an insight that node features can be recovered through a closed-form rule once graph structure is obtained.

- We propose GraphDLG, a novel approach to recover training graphs from the shared gradients and the FGL model. GraphDLG first recovers graph structures from graph embeddings with the FGL model and auxiliaries which are heterogeneous to victim’s graphs and then recovers the node features utilizing the proposed closed-form recursive rule.
- We conduct extensive experiments to validate performance of the proposed GraphDLG. The results show that our solution outperforms baselines by more than 5.46% in node features (by MSE) and more than 25.04% in graph structure (by AUC), *i.e.* existing approaches for other data types perform poorly, especially in recovering graph structures (shown in Tab. 5). Besides, an ablation study demonstrates that tackling the heterogeneity between the auxiliary graphs and victim’s graphs also improves GraphDLG’s effectiveness.

In the rest of this paper, we first review the representative related work in Sec. 2 and introduce preliminaries in Sec. 3. Then, we present our GraphDLG approach in Sec. 4. Finally, we show the experimental results in Sec. 5 and conclude this work in Sec. 6.

2 RELATED WORK

Our study is mainly related to two lines of research: (i) *the federated graph learning (FGL)* and (ii) *the deep leakage from gradients (DLG)*. We review representative works in each research area as follows.

2.1 Federated Graph Learning

Federated Graph Learning (FGL) addresses learning tasks where graph datasets are distributed across multiple data owners while ensuring compliance with strict data regulations such as GDPR [35] and CCPA [6], which prohibit the direct data sharing. Existing research in FGL can be divided into three categories based on the level of the graph data held by clients, *i.e.* (i) *Graph-level FGL* [10, 11, 17, 31, 33, 37, 46], (ii) *Subgraph-level FGL* [22, 24, 47, 52] and (iii) *Node-level FGL* [14, 28]. In this work, we focus on the *Graph-level FGL*, a common scenario for various real-world applications.

Next, we review the representative prior works in *Graph-level FGL*, which mainly focus on addressing the data heterogeneity (*a.k.a. non-i.i.d.*) and the data privacy. GCFL [46] designs a gradient sequence based clustering mechanism to enhance model aggregation among heterogeneous graphs. FedSpray [10] enables alignment of global structure proxies among multiple graphs in a personalized manner. Besides, some works focus on privacy-preserving techniques in FGL as well. For example, FKGE [33] proposes an aggregation mechanism for federated graph embedding, using differential privacy to preserve the privacy of raw graph data. Though prior works [3, 12, 17] emphasize the importance of privacy protection, they do not explore whether private graphs can be recovered via the shared information (e.g., gradients) in FGL, which is a crucial issue helps us to identify the privacy risk. In this work, we study whether private graphs can be recovered through gradients and aim to fill gaps in understanding privacy leakage risk in FGL.

2.2 Deep Leakage from Gradients

In federated learning, recent studies [30, 51] have shown that the private training data can be recovered from shared gradients, which is known as the *deep leakage from gradient (DLG)* problem. Existing

solutions for DLG attack can be classified into two categories [53]: the *optimization-based DLG* and the *analytics-based DLG*.

In the seminal work, Zhu [59] *et al.* formally define the DLG problem and propose an optimization-based attack that treats the generated dummy data as optimized parameters, which recovers the raw data from dummy data by minimizing the differences between the gradients produced by the dummy data and the shared received gradients. iDLG [56] enhances the reconstruction by extracting labels of the target raw data, while subsequent works improve performance by employing other loss functions in recovering process [13, 40, 41]. Some solutions [16, 18, 25, 44, 50] also utilize the prior knowledge to improve the recovery ability. For example, GIAS [18] and GGL [25] optimizing a dummy latent vector rather than a dummy data and leverages the prior knowledge embedded in the pre-trained GANs. However, these solutions overlook the heterogeneous between the priors and the target data. Analytics-based solutions aim to derive a closed-form formulation that describes the relationship between shared gradients and raw data. The work in [34] demonstrates that the input to a fully connected layer can be inferred by dividing the weights' gradient by the bias gradient. R-GAP [58] subsequently proposes a closed-form recursive procedure for calculating the inputs of convolutional neural networks. Though these solutions perform well in MLPs or CNNs, which avoid extensive optimization iterations and achieve high accuracy, they can not be applied in federated graph learning, leaving the privacy risks associated with recovering graph data from its gradients unexplored. Though recent work [2, 36] for privacy leakage in FGL study the DLG for graphs, they still applies the idea for image data [59] to recover node embeddings. In this work, we explore and devise solutions to the graph-tailored DLG problem, and also use prior DLG approaches for other data types as baselines.

3 PRELIMINARIES

In this paper, we study the DLG issues in Graph-level FGL, where multiple clients jointly train graph learning model via a federated manner. We first introduce basic models and concepts in Graph-level FGL, and then illustrate the adopted threat model in this work.

3.1 Basic Graph Learning Model

Notations for Graphs. Given a set of graphs $\mathcal{G} = \{G_1, \dots, G_N\}$, each graph G_i is associated with a class label Y_i for classification. For each graph $G = (V, E)$, V and E denote the set of nodes and edges of the graph G , respectively. The node features of a graph are represented by a matrix $X \in \mathbb{R}^{|V| \times d_X}$, where d_X is the feature dimension. The edges are typically depicted by the adjacency matrix $A \in \mathbb{R}^{|V| \times |V|}$, where $A_{ij} = 1$ if two nodes v_i and v_j are connected.

Graph Neural Networks. GNNs are widely-used solutions to acquire effective representations of graphs [45, 55], which usually is followed by the use of MLPs for various downstream tasks. The main idea of GNNs is to learn node representations by propagating and aggregating neighbor information, thereby integrating both node features and the graph's topological structure. In this paper, we focus the representative *graph convolutional networks* (GCNs) [21], where the information propagation rule is defined as follows,

$$H_{l+1} = \sigma(\tilde{D}^{-\frac{1}{2}} \tilde{A} \tilde{D}^{-\frac{1}{2}} H_l W_l). \quad (1)$$

Here $H_l \in \mathbb{R}^{|V| \times d_H}$ is the node embedding matrix of the l -th layer in GCNs; $\tilde{A} = A + I_{|V|}$ is the adjacency matrix with added self connections and \tilde{D} is the corresponding degree matrix of the input graph G ; σ is the non-linear activation function, such as ReLU(\cdot). After GNNs, to obtain graph-level representation H_G from node embeddings H_l , a pooling operation $\text{Pool}(\cdot)$ is commonly used to aggregate embeddings of all nodes, which can be implemented as,

$$H_G = \text{Pool}(H_l) = \text{Pool}(\{h_{l,v} | v \in G\}), \quad (2)$$

where $h_{l,v}$ is node v 's embedding of the l -th layer. The operations mentioned above enable the capture of the entire graph's embedding, which utilizes both node features and the graph structure.

3.2 Federated Graph Learning

Graph-level FGL Setting. We consider a FGL scenario with a central server S and M clients denoted as $C = \{C_1, \dots, C_M\}$. Each client C_i holds a set of private graphs $\mathcal{G}_i = \{G_{i,1}, \dots, G_{i,N_i}\}$, where N_i is the number of local graphs and $N = \sum_{i=1}^M N_i$ is the total graphs in the federation. The FGL aims to collaboratively train a graph learning model F (*e.g.* graph classification) across M clients based on GNNs, without sharing the private raw graphs (including node features and edges). The objective of the FGL is to optimize learnable weights W in F based on $\mathcal{G}_1, \dots, \mathcal{G}_M$ and to find an optimal W^* minimizing the overall loss of all FGL clients as follows,

$$W^* = \underset{W}{\operatorname{argmin}} \sum_{i=1}^M \frac{N_i}{N} \mathcal{L}(F_i, W, \mathcal{G}_i). \quad (3)$$

Graph-level FGL Training. Generally, the training process of FGL comprises the following steps [48]: At each global epoch, each client C_i update the local model based on private dataset and send gradients ∇W_i to the server S . Then server S updates the global model weight using aggregated gradients as $W = W - \eta \sum_{i=1}^M \frac{N_i}{N} \nabla W_i$, and forwards W back to the clients for next epoch of updates. By this process, a global model that learned from all clients' data can be obtained without sharing private graphs. In the DLG problem, the shared gradients ∇W_i in training process is taken as available information for recovering the private training sample.

3.3 Threat Model

Adversary's Knowledge and Capability. In this work, we adopt the honest-but-curious adversary, who eavesdrops on the communication between the server S and any client C_i during the federated graph learning. In FGL training process, the adversary is access to: (i) the shared gradients $\nabla W_{i,i \in [M]}$ of each clients, (ii) the model parameters W at each training epoch, and (iii) an auxiliary graph dataset \mathcal{G}_{aux} as the prior knowledge. Note that the last assumption is reasonable as an adversary may be an FGL clients with local graphs or collect some public graph datasets from similar scenarios. In this work, we make a deeper understanding of information leakage from gradients in FGL under the three assumptions outlined above. As next, we formally introduce the DLG attack for graphs (*i.e.* the adversary's objective), where an adversary aims to recover the victim client's private graph based on the shared gradients in the training process of the federated graph learning.

DEFINITION 1 (DLG ATTACK FOR GRAPHS). *In FGL scenario with M clients, where each client $C_i, i \in [M]$ owns a set of graphs \mathcal{G}_i*

as its private dataset, an adversary \mathcal{A} in DLG is allowed to access to the victim client C_v 's gradients ∇W_v , the federated graph model F (i.e. model parameters W) and an auxiliary graph dataset \mathcal{G}_{aux} . Then the adversary attempts to recover node features \hat{X} and the graph structure (represented as adjacency matrix \hat{A}) close to a private graph G (i.e. the ground truth node features and graph structures) in \mathcal{G}_v .

4 METHOD

In this section, we propose GraphDLG, a novel framework to recover graphs from shared gradients in FGL (in Fig. 2). We first analyze the data leakage through gradients from the theoretical view, providing a foundation for the main idea of GraphDLG (Sec. 4.1). Next, we devise an auto-encoder to recover the graph structure that utilizes the precisely leaked graph embeddings from our analysis and the auxiliary graphs (Sec. 4.2). Finally, we integrate the recovered graph structure into the found closed-form recursive rules and propose a recovery algorithm for node features, thereby recovering an entire private graph of the victim FGL client (Sec. 4.3).

4.1 Graph Data Leakage Analysis

As mentioned above, a key challenge to recovering graphs in the DLG is that the graph structure and node features are intertwined in the gradients by the forward process in FGL. Exploring the relations between the graph structure and node features is beneficial to decoupling and recovering them. Next, we briefly review the forward process in graph-level GNNs and analyze the information leaked through the shared gradients and model parameters.

Forward Process. We begin the analysis with the model forward process, where three parts in the graph-level FGL (including GCN layers H_l , MLP layers \hat{Y} and loss function L) are calculated as:

$$H_l = \sigma_l(\hat{A} \underbrace{\sigma_{l-1}(\hat{A} \sigma_{l-2}(\hat{A} \psi(X, A) W_{l-2}) W_{l-1})}_{H_{l-2}} W_l) \quad (4)$$

$$\hat{Y} = W_{fc}(M_p H_l)^\top + W_b \quad (5)$$

$$L = \mathcal{L}(\hat{Y}, Y) \quad (6)$$

In GCN layers, we follow the widely-used model in [21] and rewrite the forward process in a recursive manner, which is more convenient for analysis. Specifically, H_l , H_{l-1} and H_{l-2} are the different GCN layers with $\hat{A} = \tilde{D}^{-\frac{1}{2}} \tilde{A} \tilde{D}^{-\frac{1}{2}}$ and $\psi(X, A)$ denotes input of the $(l-2)$ th GCN layer H_{l-2} . In MLP layers, the pooling operation (e.g. sum pooling or mean pooling) can be denoted by multiplying the matrix M_p (details in Appendix A.1). W_{fc} and W_b are parameters for the linear layer (our analysis can also be extended to multiple layers in following discussion). After that, the loss function $\mathcal{L}(\cdot)$ is calculated. In this work, we calculate the gradients of the model parameters W in each layer, i.e., $\nabla W = \frac{\partial L}{\partial W}$, through which we can derive the closed-form relations between layer inputs and the corresponding gradients for both the MLP layers and the GCN layers.

4.1.1 Leakage in MLP Layers. Firstly, we can calculate the gradients of parameters W_{fc} and W_b in the MLP layer by treating the pooling operation as matrix multiplication as follows,

$$\nabla W_{fc} = \left(\frac{\partial L}{\partial \hat{Y}} \right)^\top M_p H_l, \quad \nabla W_b = \left(\frac{\partial L}{\partial \hat{Y}} \right)^\top. \quad (7)$$

Then the pooled graph embedding $M_p H_l$, i.e., input of the MLP layer, can be recovered by any row of the gradients ∇W_{fc} and ∇W_b ,

$$M_p H_l = \nabla W_{fc}^j / \nabla W_b^j, \quad (8)$$

where ∇W_{fc}^j and ∇W_b^j denotes any row of ∇W_{fc} and ∇W_b , respectively. As for multiple MLP layers, once the last layer's input (i.e. previous layers' output) is determined, the input of the first layer can be retrieved by solving linear equations recursively $W_{fc,t} X_{t-1}^\top + W_{b,t} = X_t$ ($t = 1, \dots, l_{MLP}$). As a result, the MLP layer can easily leak its input H_G through the gradients of its parameters.

4.1.2 Leakage in GCN Layers. Next, we further study the information that might be leaked through the gradients in GCN layers. Similarly, we can derive gradients based on Eq. (4)~Eq. (6), and we have the following analytical expressions for the l -GCN layers.

LEMMA 1 (GRADIENTS IN AN l -LAYER GCN). For the GCN layers in FGL, the gradients ∇W_l , ∇W_{l-1} , ∇W_{l-2} can be formally expressed by the node embeddings from their previous layer H_{l-1} , H_{l-2} , H_{l-3} respectively and the normalized graph adjacency matrix \hat{A} ,

$$\nabla W_l = H_{l-1}^\top \hat{A}^\top (M_p^\top \frac{\partial L}{\partial \hat{Y}} W_{fc} \odot \sigma'_l) \quad (9)$$

$$\nabla W_{l-1} = H_{l-2}^\top \hat{A}^\top (\hat{A}^\top (M_p^\top \frac{\partial L}{\partial \hat{Y}} W_{fc} \odot \sigma'_l) W_l^\top \odot \sigma'_{l-1}) \quad (10)$$

$$\nabla W_{l-2} = H_{l-3}^\top \hat{A}^\top (\hat{A}^\top (\hat{A}^\top (M_p^\top \frac{\partial L}{\partial \hat{Y}} W_{fc} \odot \sigma'_l) W_l^\top \odot \sigma'_{l-1}) W_{l-1}^\top \odot \sigma'_{l-2}) \quad (11)$$

where σ' represents the derivative of the activate function σ . The term $\frac{\partial L}{\partial \hat{Y}}$ in Eq. (9) can be derived from Eq. (7), while M_p , W_{fc} and W_l are already known model parameters. The proof of Lemma 1 is in Appendix A.2. The gradients of activate function σ'_l can be derived from the output of l -th layer and more details are in Appendix A.1.

Observing repeated components for each layer in GCNs, we can rewrite them and derive a closed-form recursive rule as follows.

$$\nabla W_l = H_{l-1}^\top \mathbf{r}_l, \quad \mathbf{r}_l = \hat{A}^\top (M_p^\top \frac{\partial L}{\partial \hat{Y}} W_{fc} \odot \sigma'_l) \quad (12)$$

$$\nabla W_{l-1} = H_{l-2}^\top \mathbf{r}_{l-1}, \quad \mathbf{r}_{l-1} = \hat{A}^\top (\mathbf{r}_l W_l^\top \odot \sigma'_{l-1}) \quad (13)$$

$$\nabla W_{l-2} = H_{l-3}^\top \mathbf{r}_{l-2}, \quad \mathbf{r}_{l-2} = \hat{A}^\top (\mathbf{r}_{l-1} W_{l-1}^\top \odot \sigma'_{l-2}) \quad (14)$$

For the i th layer, we conjecture that a similar equation still holds,

$$\nabla W_i = H_{i-1}^\top \mathbf{r}_i, \quad \mathbf{r}_i = \hat{A}^\top (\mathbf{r}_{i+1} W_{i+1}^\top \odot \sigma'_i), i = 1, \dots, l-1. \quad (15)$$

In this work, we can prove the above conjecture and derive the following recursive rule for GCN layers (proof in Appendix A.2).

THEOREM 1 (RECURSIVE RULE FOR GRADIENTS). The gradients ∇W_i in GCN layers can be depicted by its input embedding H_{i-1} and a coefficient matrix \mathbf{r}_i in a closed-form recursive equation, i.e.,

$$\nabla W_i = H_{i-1}^\top \mathbf{r}_i, \quad (16)$$

where the coefficient matrix \mathbf{r}_i is defined as follows,

$$\mathbf{r}_i = \begin{cases} \hat{A}^\top (M_p^\top \frac{\partial L}{\partial \hat{Y}} W_{fc} \odot \sigma'_i), & i = l \\ \hat{A}^\top (\mathbf{r}_{i+1} W_{i+1}^\top \odot \sigma'_i), & i = 1, \dots, l-1 \end{cases} \quad (17)$$

Theorem 1 implies that once graph structure \hat{A} is obtained, \mathbf{r}_i can be then calculated by solving a linear equations, $\nabla W_i^\top = \mathbf{r}_i^\top H_{i-1}$ and then we can recursively compute \mathbf{r}_i and H_i alternatively until input of the first GCN layer H_0 (i.e., node features X) is recovered.

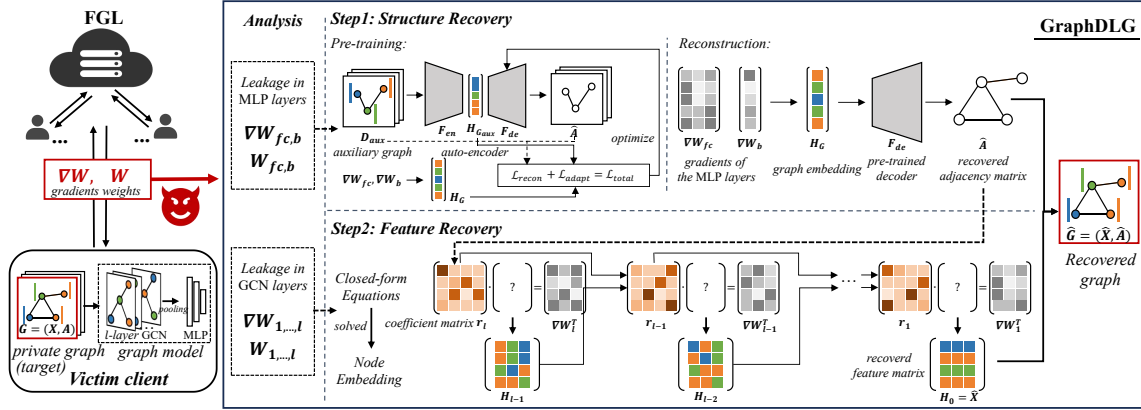


Figure 2: Overview of GraphDLC. Firstly, a learned decoder can recover graph structure from graph embeddings leaked in MLP layers’ gradients. Then, node features can be recovered by recursively solving closed-form equations. Finally, the attacker obtained the whole graph.

4.1.3 Takeaways. Above analysis provide us two crucial insights. (i) *Graph embeddings H_G can be easily recovered from gradients.* Thus, we can utilize the H_G , an intermediate closer to the original graph, rather than the output loss, to recover the original graph. (ii) *Theorem 1 not only decouples node features and graph structure in gradients but also establishes a recovery order for them.* This simplification aids in the task of simultaneously recovering both graph structure and node features from gradients. Based on the two results, we introduce our GraphDLC, which first recovers the graph structure from the easily obtained graph embeddings H_G (in Sec. 4.2) and then recovers the node features using Theorem 1 (in Sec. 4.3).

4.2 Structure Recovery with Hetero-Priors

Following the established recovery order, we design an auto-encoder based on FGL models and use its decoder to transform obtained graph embeddings H_G (in Sec. 4.1) into the graph structure \hat{A} .

Main idea. As above, we have successfully recovered the graph embeddings H_G (*i.e.*, final output of GCN layers), which integrates both the graph structure and node features. Thus, we can extract the graph structure from H_G . Specifically, we design an auto-encoder to fully utilize the knowledge in the FGL model and priors in auxiliary graphs \mathcal{G}_{aux} , where the FGL model is fixed as the encoder to transform the original input graph into the embeddings H_G and then the decoder is with the capability to recover the graph structure from the graph embeddings. We further design an adapter to handle the heterogeneity between the prior and target graphs.

Auto-Encoder for Graph Structure. We introduce the proposed auto-encoder to recover the graph structure as follows.

$$H_G = F_{en}(X, A), \quad \hat{A} = F_{de}(H_G) \quad (18)$$

(i) *Encoder Module:* Here $F_{en}(\cdot)$ is the encoder, which shares the same parameters as the federated graph model in FGL except for the MLP layers. This design aims to utilize the knowledge in the federated graph model to enhance recovery. The encoder takes the graph’s node features X and adjacency matrix A as inputs and outputs the graph embedding H_G . (ii) *Decoder Module:* Here $F_{de}(\cdot)$ is the decoder which takes graph embedding H_G as input and outputs the recovered adjacency matrix \hat{A} . We employ a three-layer MLP

ending with the Sigmoid function as the decoder to transform the graph embedding vector back to the adjacency matrix. (iii) *Loss function:* We use the auxiliary graph datasets \mathcal{G}_{aux} to train the decoder F_{de} with the reconstruction loss as follows,

$$L_{recon} = \frac{1}{|\mathcal{G}_{aux}|} \sum_{(X, A) \in \mathcal{G}_{aux}} \|F_{de}(F_{en}(X, A)) - A\|^2 \quad (19)$$

Thereby, the GraphDLC can use the auxiliary priors \mathcal{G}_{aux} to train the decoder and recover the graph structure of the target graphs.

Utilizing Heterogeneous Priors. As we have obtained the ground-truth embeddings H_G from target graphs \mathcal{G}_v , we can align the distribution of the target graphs \mathcal{G}_v and the auxiliary graphs \mathcal{G}_{aux} using their graph embeddings from the same FGL model instead of the unavailable private original graphs. Specifically, we use the domain adaption [32] and adopt the widely-used *Maximum Mean Discrepancy* (MMD) as the distance metric to minimize divergences between graph embeddings from \mathcal{G}_{aux} and \mathcal{G}_v , so that the decoder trained on auxiliaries \mathcal{G}_{aux} can still perform well on \mathcal{G}_v . Formally, the distance metric $MMD(\cdot, \cdot)$ is defined as follows,

$$MMD(\mathcal{G}_i, \mathcal{G}_j) = \left\| \sum_{G_{i,k} \in \mathcal{G}_i} \phi(H_{G_{i,k}}) / |\mathcal{G}_i| - \sum_{G_{j,k} \in \mathcal{G}_j} \phi(H_{G_{j,k}}) / |\mathcal{G}_j| \right\|, \quad (20)$$

where ϕ denotes the mapping to a Reproducing Kernel Hilbert Space (RKHS). We add $MMD(\mathcal{G}_{aux}, \mathcal{G}_v)$ as the regularization to the reconstruction loss and the total loss function is as follows,

$$L_{total} = L_{recon} + \lambda MMD(\mathcal{G}_{aux}, \mathcal{G}_v) \quad (21)$$

Here, λ serves as the weight coefficient for normalizing L_{adapt} .

Discussion. Next, we provide a brief discussion on the auxiliary dataset \mathcal{G}_{aux} . A key advantage of our approach is that it does not require auxiliary graphs to follow the same distribution as the victim’s dataset, making it broadly applicable in practice. Specifically, an attacker may exploit its local training graphs, publicly available graph datasets, or randomly generated graph structures. To validate this flexibility, we conduct experiments to examine three auxiliary data scenarios, *i.e.* auxiliaries from the same distribution, from heterogeneous distributions, and from random generation.

Algorithm 1: Graph Node Features Recovery (GNFR)

```

input :FGL models  $W$ , victim clients gradients  $\nabla W$ ;
        recovered adjacency matrix  $\hat{A}$ ;
output: The victim's node features  $\hat{X}_0$ ;
1  $\tilde{A} = \hat{A} + I$ ,  $\tilde{A} = \tilde{D}^{-\frac{1}{2}} \tilde{A} \tilde{D}^{-\frac{1}{2}}$ ;
2 for  $layer k \leftarrow l$  to 1 do
3   if  $k == l$  then
4     Initialized  $\mathbf{r}_k$  using Eq. (7) and Eq. (12);
5   else
6     Derive  $\sigma_k$  from  $\hat{X}_k$ ;
7      $\mathbf{r}_k \leftarrow \tilde{A}^\top (\mathbf{r}_{k+1} W_{k+1}^\top \odot \sigma_k)$ ;
8      $B \leftarrow flatten(\nabla W_k^\top)$ ;
9      $R \leftarrow \mathbf{r}_k^\top \otimes I_{d_{\hat{X}_{k-1}}}$ ;
10    Solving linear equations  $Rx = B$ ;
11     $\hat{X}_{k-1} \leftarrow unflatten(x)$ ;
12 return  $\hat{X}_0$ ;

```

4.3 Feature Recovery via Closed-form Rules

In this subsection, we introduce the *Graph Node Features Recovery* (GNFR) algorithm, which utilizes the estimated graph structure \hat{A} to recover the node features \hat{X} based on our recursive closed-form rule in Theorem 1. Specifically, we illustrate the graph node features recovery algorithm in Algorithm 1. The main idea of Algorithm 1 is that if we can recursively calculate node embeddings in each GCN layer of the FGL, we can ultimately recover the original node features \hat{X}_0 . The algorithm starts from the final GCN layer and proceeds layer by layer. For the k_{th} GCN layer, the coefficient matrix \mathbf{r}_k is computed based on values in the $(k+1)_{th}$ layer (in lines 3–7). In lines 8–11, we calculate node embedding matrix of the previous layer (*i.e.* \hat{X}_{k-1}) by solving linear equations. To convert the matrix equation into a standard linear system, we flatten ∇W_k^\top into a vector in line 8 and convert the coefficient matrix into $\mathbf{r}_k^\top \otimes I_{d_{\hat{X}_{k-1}}}$ in line 9. Here \otimes denotes the Kronecker product and $I_{d_{\hat{X}_{k-1}}}$ is the identity matrix with dimensions $d_{\hat{X}_{k-1}} \times d_{\hat{X}_{k-1}}$, and $d_{\hat{X}_{k-1}}$ is the last dimension of \hat{X}_{k-1} . After solving the standard linear equations in line 10, we reshape the vectorized results x to obtain the node embedding matrix \hat{X}_{k-1} in line 11. Through the above iterative process in Algorithm 1, we can effectively reconstruct node features, ultimately retrieving the complete graph from the shared gradients.

5 EXPERIMENTS

We conduct extensive experiments to verify the effectiveness of proposed GraphDLG, aiming to answer the following three questions. **Q1:** State-of-the-art solutions are not tailored for the graph data, prompting us to evaluate their performance on graphs, *i.e.*, can GraphDLG achieve better performance for graph recovery? **Q2:** Prior solutions overlook the heterogeneity between priors and target data, so we question that *how heterogeneity affects graph recovery and whether our GraphDLG can improve recovery by the adapter designed to handle heterogeneous priors?* **Q3:** Existing defense methods (*e.g.* gradient compression [59] and differential privacy [27])

are commonly employed to counter the DLG attacks, so we question that *to what extent are they against the proposed GraphDLG?*

5.1 Experimental Setup

Datasets. We use five graph classification datasets [29], including *(i) Molecule datasets* (MUTAG, PTC_MR, and AIDS), where each node represents an atom (with a one-hot vector as its feature), and edges denote chemical bonds. *(ii) Bio-informatics datasets* (ENZYME and PROTEINS), where each node represents an amino acid with features indicating type and edges connecting neighboring amino acids. Unlike previous experimental setups in DLG [18, 25] which randomly split the graph datasets, we adopt the Dirichlet distribution to establish the heterogeneity between auxiliaries and targets. In ablation studies, we further conduct experiments in two scenarios: *(i)* target and auxiliary graphs are from different datasets and *(ii)* the auxiliary graphs are randomly generated.

Baselines. We compare the proposed GraphDLG with eight baselines for DLG problem, including Random, DLG [59], iDLG [56], InverGrad [13], GI-GAN [18, 25], GRA-GFA [2], TabLeak [38] and Graph Attacker [36]. More details of baselines are in Appendix A.4.

Configurations. In following experiments, we implement global graph learning model as a two-layer GCN with a linear layer as the classifier. The hidden size of the GCN layers is set to 16. For our proposed GraphDLG, the hidden size of F_{de} is set to [100, 250], and the output size is determined by the maximum number of nodes in the target graphs. We use the identity function to approximate ϕ since the encoder has projected the graph feature into a high-dimension space. We set λ to 0.2 based on a parameter search, and the auto-encoder model is optimized using Adam with a learning rate of 0.001. For any baselines that include optimization process, the maximum number of recovery iterations is set to 100. Other hyperparameters follow the settings reported in the original paper. Due to limited space, more setups are described in Appendix A.3 and more results of various GCN configurations (including batch sizes, GCN layers and hidden sizes) are presented in Appendix A.6.

Evaluation Metrics. *(i) Node Features:* we use the mean square error (MSE) to evaluate recovery performance. Since node features represent node types, we use node class accuracy (ACC) to evaluate results semantically. *(ii) Graph Structure:* we employ area under the ROC curve (AUC) and average precision (AP) as metrics, which are widely used to measure binary classification performance across various thresholds. For a straightforward interpretation, we also present the accuracy of edges using a threshold of 0.5. *Specifically, a lower MSE and a higher AUC indicate better recovery performance.*

5.2 Performance Comparison

To answer **Q1**, we compare our method with eight baselines in terms of recovering graph structure and features. The results are presented in Tab. 1. Overall, our GraphDLG outperforms the baselines in structure and feature recoveries, with a reduction of over 5.46% in node features by MSE and an increase of over 25.04% in the adjacency matrix by AUC. A case study is also provided in Tab. 2 to demonstrate this superiority. Detailed analysis is as follows.

Results on Graph Structure. Regarding the graph structure recovery, significant improvements are observed across all metrics

Table 1: Comparison of performance on feature and structure recoveries between GraphDLC and baselines. The best result is bold and the second result is underlined.

Dataset	Method	Node Feature		Adjacency Matrix	
		MSE	ACC(%)	AUC	AP
MUTAG	Random	0.3366	13.03	0.4933	0.1301
	DLG [59]	1.2265	18.47	0.5226	0.1415
	iDLG [56]	1.1063	19.66	0.5243	0.1409
	InverGrad [13]	0.9164	28.04	0.5183	0.1417
	GI-GAN [18, 25]	<u>0.1053</u>	51.86	0.5081	0.1246
	GRA-GRF [2]	0.1082	<u>71.37</u>	0.4891	0.1255
	TabLeak [38]	0.3914	21.16	0.5323	0.1436
	Graph Attacker [36]	1.0366	27.74	0.5223	0.1287
	GraphDLC (ours)	0.0844	74.35	0.9042	0.7556
PTC_MR	Random	0.3334	6.95	0.4858	0.1661
	DLG [59]	1.0289	12.33	0.5372	0.1992
	iDLG [56]	1.0608	11.13	0.5307	0.1864
	InverGrad [13]	0.9154	16.19	0.5469	0.1939
	GI-GAN [18, 25]	0.0586	5.81	0.4919	0.1529
	GRA-GRF [2]	<u>0.0372</u>	<u>70.45</u>	0.4753	0.1506
	TabLeak [38]	0.3308	9.75	0.5656	0.2040
	Graph Attacker [36]	0.9893	15.15	0.5495	0.1779
	GraphDLC (ours)	0.0329	72.53	0.8893	0.6808
AIDS	Random	0.3329	2.44	0.5022	0.2057
	DLG [59]	1.0834	5.78	0.5475	0.2192
	iDLG [56]	1.1559	5.99	0.5437	0.2187
	InverGrad [13]	0.8535	8.79	0.5526	0.2221
	GI-GAN [18, 25]	0.0262	6.17	0.5072	0.1793
	GRA-GRF [2]	<u>0.0238</u>	<u>53.79</u>	0.4754	0.1719
	TabLeak [38]	0.3015	3.67	0.5505	0.2229
	Graph Attacker [36]	0.9150	7.86	0.5383	0.1901
	GraphDLC (ours)	0.0225	62.18	0.7677	0.5113
ENZYMEs	Random	0.3315	32.53	0.5000	0.1725
	DLG [59]	2.8092	37.43	0.5273	0.1834
	iDLG [56]	1.5751	36.40	0.5263	0.1817
	InverGrad [13]	1.1449	40.14	0.5290	<u>0.1836</u>
	GI-GAN [18, 25]	<u>0.2083</u>	41.19	0.4978	0.1627
	GRA-GRF [2]	0.2229	52.26	0.4819	0.1595
	TabLeak [38]	0.5706	34.88	0.5310	0.1835
	Graph Attacker [36]	1.3590	40.64	0.5251	0.1734
	GraphDLC (ours)	0.1772	60.60	0.6615	0.3911
PROTEINS	Random	0.3354	31.71	0.4969	0.1733
	DLG [59]	1.5237	38.05	0.5286	0.1879
	iDLG [56]	1.4736	36.67	0.5288	0.1875
	InverGrad [13]	1.1160	41.47	<u>0.5301</u>	<u>0.1889</u>
	GI-GAN [18, 25]	<u>0.2192</u>	<u>49.15</u>	0.5123	0.1710
	GRA-GRF [2]	0.2198	40.44	0.4802	0.1603
	TabLeak [38]	0.5904	35.11	0.5255	0.1856
	Graph Attacker [36]	1.2923	42.51	0.5242	0.1745
	GraphDLC (ours)	0.1935	62.23	0.6630	0.3744

compared to baselines. As depicted in Tab. 1, the AUC scores of the baselines are around 0.5 across all datasets, indicating performance akin to random guessing, while our proposed GraphDLC achieves AUC values ranging from 0.66 to 0.9. This validates the effectiveness of our design in Sec. 4, where we focus on initially recovering only the graph structure with leaked graph embeddings and priors, thereby simplifying the recovery process. As baseline methods rely on iterative optimizations to recover edges from gradients, this task remains highly challenging due to the mixed feature and structural information in gradients, leading to poor performance.

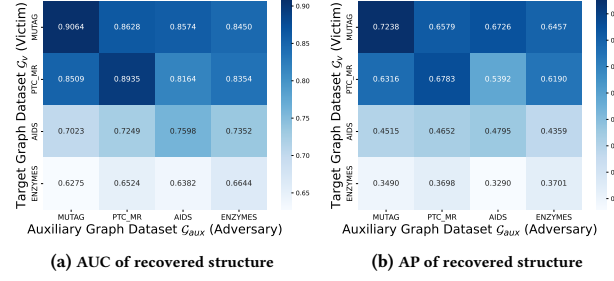


Figure 3: Structure recovery performance with hetero-priors, i.e. target and auxiliary graphs datasets are different.

Results on Node Features. We have observed notable improvements in feature recovery, as shown in Tab. 1, particularly due to a reduction in MSE. Methods employing priors, such as GI-GAN, GRA-GRF, and our proposed GraphDLC, consistently outperform those based solely on optimization process with gradients, reducing MSE errors by at least 0.1×. Among these three methods, our GraphDLC stands out by solving closed-form equations that clarify the relationship between gradients and features, leading to an average MSE reduction of 17.6%. Our method also achieves the highest accuracy in terms of ACC over all datasets, particularly excelling with the AIDS dataset, which includes 37 node types.

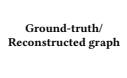
Case Study. The visualizations of graph recovery in Tab. 2 demonstrate the strong capability of our approach in recovering the graph data. Specifically, the AUC of our GraphDLC is 0.96, whereas others range from 0.49~to 0.60. From the visualizations, we can observe that other baselines tend to reconstruct fully connected graphs, which are far away from the ground-truth graph structure to be reconstructed. Furthermore, the visualization results support that higher AUC, AP, and ACC metrics consistently correspond to better graph structure recovery performance. Similar observations can also be found in additional cases, as shown in Appendix A.5.

5.3 Ablation Studies

To answer Q2, we utilize four datasets to explore more heterogeneous setting scenarios, where the adversary employs GraphDLC with diverse auxiliary graphs (e.g. from MUTAG) to recover victim clients' private graphs from a different dataset (e.g. AIDS). Unlike previous studies, which only used prior auxiliaries from the same target dataset, we fill the gap by exploring the effects of heterogeneous priors. Our findings show that this heterogeneity affects the recovery of graph data, and we further confirm that our designed adapter enhances recovery effectiveness in such scenarios.

Impact of Hetero-Priors. We assess the recovery performance using GraphDLC without the designed adapter to determine the impact of heterogeneous priors. As depicted in Fig. 3, the AUC and AP metrics of recovered structures reach their peak values for the same target dataset only when the target and auxiliary datasets are drawn from the same distribution (i.e., values along the diagonal of the heatmap), showing that diversity between priors and target graphs could hinder the recovery of the graph structure. We also observe that GraphDLC consistently achieves higher AUC and AP

Table 2: Visualization of the recovery performance for GraphDLG and baselines.

		Random	DLG	iDLG	InverGrad	GI-GAN	GRA-GRF	Tableak	Graph-Attacker	GraphDLG (ours)
Node Feature	MSE/ACC(%)	0.3059/7.14	1.3186/14.29	1.0636/21.43	0.8969/35.71	0.1008/57.14	0.1068/78.57	0.4203/21.43	1.0295/28.57	0.0816/78.57
Adjacency Matrix	AUC/AP/ACC(%)	0.4926/0.1604/46.94	0.6058/0.1902/66.33	0.5108/0.1599/59.69	0.4865/0.1585/44.90	0.5120/0.1563/17.35	0.5863/0.1817/53.06	0.5382/0.1614/74.49	0.4978/0.1525/31.12	0.9622/0.8832/93.88
Ground-truth/ Reconstructed graph										

scores than all other baselines, when using various datasets (MUTAG, PTC_MR, AIDS, ENZYMEs) as the auxiliary graphs.

Results on Random Auxiliary Graph. We conduct experiments where the MUTAG dataset serves as target dataset, and the auxiliaries are randomly generated graphs. Specifically, we employ the widely-used Erdős–Rényi graph model [8] to generate graph structures ($\mathcal{G}(0.5)$ denotes that any two nodes are connected independently with a probability of 0.5), while node features are sampled from Gaussian or Uniform distributions. As shown in Tab. 3, when the MUTAG auxiliary dataset is replaced with these randomly generated ones, the adjacency matrix accuracy of our method decreases slightly from 93.41% to 87.73% and it still outperforms other baselines. Moreover, the accuracy of node features of our GraphDLG remains stable, showing its robustness in feature recovery against variations in recovery results of the graph structures.

Table 3: Results on randomly generated auxiliary graphs.

Auxiliary Feature	Auxiliary Structure	Node Feature	Adjacency Matrix
		MSE ACC(%)	AUC AP ACC(%)
MUTAG	MUTAG	0.0844 74.35	0.9042 0.7556 93.41
$\mathcal{N}(0, 1)$	$\mathcal{G}(0.1)$	0.0844 74.35	0.5917 0.1691 87.73
$\mathcal{N}(0, 1)$	$\mathcal{G}(0.05)$	0.0844 74.35	0.6155 0.1765 87.73
$\mathcal{U}[-1, 1]$	$\mathcal{G}(0.1)$	0.0844 74.35	0.5762 0.1645 87.73
$\mathcal{U}[-1, 1]$	$\mathcal{G}(0.05)$	0.0844 74.35	0.6080 0.1862 87.73

Effectiveness of Adapter. Since the adapter primarily impacts structure recovery, we present the results of an ablation study on the recovered structure in Tab. 4. By introducing the adapter L_{adapt} into our proposed method, we observe higher AUC and AP values across all settings, with increases of up to 5.19% in AUC and up to 16.43% in AP. This demonstrates the effectiveness and robustness of the proposed regularization, which reduces the disparity between target and auxiliary graphs, allowing the decoder to perform better on target graphs. The above observations suggest that the graph data leakage from gradients is risky, even when target and auxiliary graphs are from heterogeneous datasets.

5.4 Evaluation under Defenses

To answer Q3, we evaluate the performance of GraphDLG under two commonly used defenses: (i) Gradient compression[59], which prunes small values in gradients with prune ratio p ; (ii) Differential privacy[27], which adds noise to gradients, and here we use Laplacian noise with variance σ . The results are shown in Fig. 4, where solid lines denote MSE and dashed lines denote ACC.

Defense with Gradient Compression. The results are in Fig. 4a indicate that the performance of feature recovery only exhibits a noticeable decrease when the prune ratio reaches as high as 0.99. However, even with a high prune ratio, it is difficult to observe a

Table 4: Ablation results on the impact of adapter in GraphDLG.

Targets	Auxiliaries	Method	AUC	AP
MUTAG	PTC_MR	w/o L_{adapt}	0.8628	0.6579
		GraphDLG (ours)	0.8778	0.6898
	AIDS	w/o L_{adapt}	0.8574	0.6726
PTC_MR	ENZYMEs	w/o L_{adapt}	0.8589	0.6833
		GraphDLG (ours)	0.8604	0.6522
	MUTAG	w/o L_{adapt}	0.8509	0.6316
AIDS		GraphDLG (ours)	0.8543	0.6348
	AIDS	w/o L_{adapt}	0.8164	0.5392
	ENZYMEs	w/o L_{adapt}	0.8588	0.6278
AIDS	MUTAG	w/o L_{adapt}	0.8354	0.6190
		GraphDLG (ours)	0.8614	0.6447
	ENZYMEs	w/o L_{adapt}	0.7023	0.4515
ENZYMEs	MUTAG	w/o L_{adapt}	0.7249	0.4652
		GraphDLG (ours)	0.7561	0.4830
	PTC_MR	w/o L_{adapt}	0.7352	0.4359
AIDS		GraphDLG (ours)	0.7416	0.4401
	MUTAG	w/o L_{adapt}	0.6275	0.3490
		GraphDLG (ours)	0.6278	0.3499
PTC_MR	ENZYMEs	w/o L_{adapt}	0.6524	0.3698
		GraphDLG (ours)	0.6562	0.3795
AIDS	MUTAG	w/o L_{adapt}	0.6382	0.3290
		GraphDLG (ours)	0.6555	0.3727

performance drop in structure recovery, as shown in Fig. 4c. This suggests that gradient compression has limited effectiveness against GraphDLG, potentially because the small values in gradients do not play a primary role in the privacy leakage exploited by GraphDLG.

Defense with Differential Privacy. Fig. 4b and Fig. 4d are results of different noise variances, where a greater variance means adding more noise, *i.e.*, a higher level of privacy protection. It is evident that as the noise level increases, the reconstruction performance decreases, particularly concerning the ACC of node features. Yet, the decrease in AP and ACC of recovered graph structure is not pronounced, indicating that while differential privacy may be less effective in protecting graph structures than node features, requiring stronger defense designs. We further discuss the potential defense methods for GraphDLG in Appendix A.7.

6 CONCLUSION

In this paper, we systematically study the deep leakage from gradients (DLG) in federated graph learning (FGL). Firstly, we uncover the relationship between graph structure and node features in DLG on graphs through the closed-form rules. Then, we propose

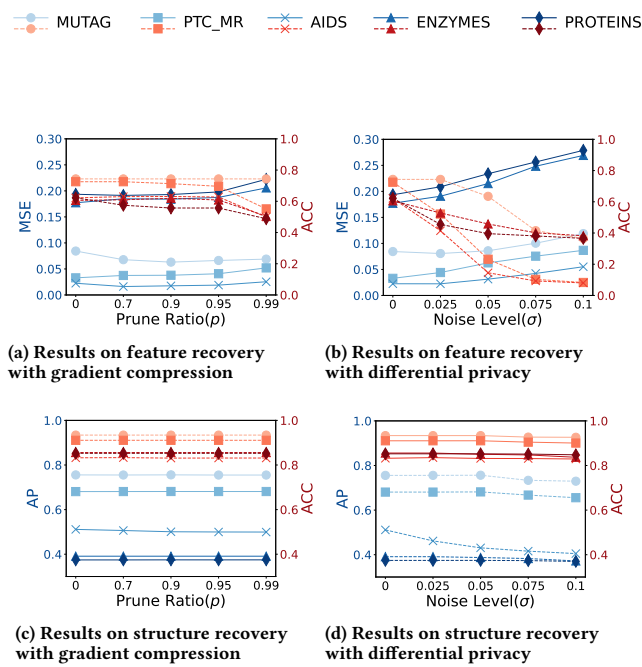


Figure 4: The effectiveness of different defense strategies.

a novel framework, GraphDLC, to recover the original graph structure and node features of private training graphs from shared gradients in FGL. GraphDLC advances the state-of-the-art by successfully disentangling structural and feature information from gradients based on the derived closed-form recursive rules. We further enhance the reconstruction performance by incorporating the auto-encoder model with an adaptation regularization designed to leverage the heterogeneous auxiliary graph dataset. Extensive experiments on five datasets demonstrate significant performance improvements compared with existing works, highlighting the substantial risks of data leakage from gradients in graph-level FGL.

REFERENCES

- [1] Nicola De Cao and Thomas Kipf. 2018. MolGAN: An implicit generative model for small molecular graphs. *ICML Workshop* (2018).
- [2] Jinyin Chen, Minying Ma, Haonan Ma, Haibin Zheng, and Jian Zhang. 2024. An Empirical Evaluation of the Data Leakage in Federated Graph Learning. *IEEE Trans. Netw. Sci. Eng.* 11, 2 (2024), 1605–1618.
- [3] Ruonan Chen, Ye Dong, Yizhong Liu, et al. 2025. FLock: Robust and Privacy-Preserving Federated Learning based on Practical Blockchain State Channels. In *WWW*. ACM, 884–895.
- [4] Edward Choi, Mohammad Taha Bahadori, Le Song, Walter F. Stewart, and Jiemeng Sun. 2017. GRAM: Graph-based Attention Model for Healthcare Representation Learning. In *KDD*. ACM, 787–795.
- [5] Limeng Cui, Haeseung Seo, Maryam Tabar, Fenglong Ma, Suhang Wang, and Dongwon Lee. 2020. DETERRENT: Knowledge Guided Graph Attention Network for Detecting Healthcare Misinformation. In *KDD*. ACM, 492–502.
- [6] Lydia de la Torre. 2018. A guide to the california consumer privacy act of 2018. In *Available at SSRN 3275571*.
- [7] Jieren Deng, Yijue Wang, Ji Li, Chenghong Wang, Chao Shang, Hang Liu, Sangthavar Rajasekaran, and Caiwen Ding. 2021. TAG: Gradient Attack on Transformer-based Language Models. In *EMNLP*. ACL, 3600–3610.
- [8] Paul Erdős and Alfred Rényi. 1960. On the evolution of random graphs. *Publ. Math. Inst. Hungar. Acad. Sci.* 5 (1960), 17–61.
- [9] Dongqi Fu, Wenxuan Bao, Ross Maciejewski, et al. 2023. Privacy-Preserving Graph Machine Learning from Data to Computation: A Survey. *SIGKDD Explor.* 25, 1 (2023), 54–72.
- [10] Xingbo Fu, Zihan Chen, Binchi Zhang, Chen Chen, et al. 2024. Federated Graph Learning with Structure Proxy Alignment. In *KDD*. ACM, 827–838.
- [11] Xinyu Fu and Irwin King. 2023. FedHGN: a federated framework for heterogeneous graph neural networks. In *IJCAI*. 3705–3713.
- [12] Xingbo Fu, Binchi Zhang, Yushun Dong, Chen Chen, et al. 2022. Federated Graph Machine Learning: A Survey of Concepts, Techniques, and Applications. *SIGKDD Explor.* 24, 2 (2022), 32–47.
- [13] Jonas Geiping, Hartmut Bauermeister, et al. 2020. Inverting gradients-how easy is it to break privacy in federated learning. In *NeurIPS*.
- [14] Zhuoning Guo, Duanyi Yao, Qiang Yang, et al. 2024. HiFGL: A Hierarchical Framework for Cross-silo Cross-device Federated Graph Learning. In *KDD*. ACM, 968–979.
- [15] Samyak Gupta, Yangsibo Huang, Zexuan Zhong, Tianyu Gao, et al. 2022. Recovering private text in federated learning of language models. In *NeurIPS*.
- [16] Ali Hatamizadeh, Hongxu Yin, Holger R Roth, Wenqi Li, et al. 2022. Gradvit: Gradient inversion of vision transformers. In *CVPR*. 10021–10030.
- [17] Kai Hu, Jiasheng Wu, Yaogen Li, Meixia Lu, et al. 2022. Fedgcn: Federated learning-based graph convolutional networks for non-euclidean spatial data. *Mathematics* 10, 6 (2022), 1000.
- [18] Jinwoo Jeon, Jaechang Kim, Kangwook Lee, Sewoong Oh, and Jungseul Ok. 2021. Gradient inversion with generative image prior. In *NeurIPS*.
- [19] Yilun Jin, Kai Chen, and Qiang Yang. 2023. Transferable Graph Structure Learning for Graph-based Traffic Forecasting Across Cities. In *KDD*. ACM.
- [20] Peter Kairouz, H Brendan McMahan, et al. 2021. Advances and open problems in federated learning. *Found. Trends Mach. Learn.* 14, 1–2 (2021), 1–210.
- [21] Thomas N. Kipf and Max Welling. 2017. Semi-Supervised Classification with Graph Convolutional Networks. In *ICLR*.
- [22] Anran Li, Yuanyuan Chen, Jian Zhang, Mingfei Cheng, Yihao Huang, et al. 2024. Historical Embedding-Guided Efficient Large-Scale Federated Graph Learning. *SIGMOD* 2, 3 (2024), 144.
- [23] Han Li, Dan Zhao, and Jianyang Zeng. 2022. KPGT: Knowledge-Guided Pre-training of Graph Transformer for Molecular Property Prediction. In *KDD*. ACM, 857–867.
- [24] Xunkai Li, Zhengyu Wu, Wentao Zhang, Yinlin Zhu, et al. 2023. FedGTA: Topology-aware Averaging for Federated Graph Learning. *Proc. VLDB Endow.* 17, 1 (2023), 41–50.
- [25] Zhuohuang Li, Jiaxin Zhang, Luyang Liu, et al. 2022. Auditing privacy defenses in federated learning via generative gradient leakage. In *CVPR*. 10132–10142.
- [26] Rui Liu, Pengwei Xing, Zichao Deng, Anran Li, et al. 2024. Federated Graph Neural Networks: Overview, Techniques and Challenges. *IEEE Trans. Neural Networks Learn. Syst.* (2024).
- [27] H. Brendan McMahan, Daniel Ramage, Kunal Talwar, and Li Zhang. 2018. Learning Differentially Private Recurrent Language Models. In *ICLR*.
- [28] Chuizhang Meng, Sirisha Rambhatla, and Yan Liu. 2021. Cross-Node Federated Graph Neural Network for Spatio-Temporal Data Modeling. In *KDD*. ACM, 1202–1211.
- [29] Christopher Morris, Nils M. Kriege, Franka Bause, Kristian Kersting, Petra Mutzel, and Marion Neumann. 2020. TUDataset: A collection of benchmark datasets for learning with graphs. In *ICML Workshop*.
- [30] Virajji Mothukuri, Reza M Parizi, Seyedamin Pouriyeh, Yan Huang, et al. 2021. A survey on security and privacy of federated learning. *Future Gener. Comput. Syst.* 115 (2021), 619–640.
- [31] Chenglu Pan, Jiarong Xu, Yue Yu, Ziqi Yang, et al. 2024. Towards Fair Graph Federated Learning via Incentive Mechanisms. In *AAAI*. 14499–14507.
- [32] Sinno Jialin Pan, James T. Kwok, and Qiang Yang. 2008. Transfer Learning via Dimensionality Reduction. In *AAAI*. 677–682.
- [33] Hao Peng, Haoran Li, Yangqiu Song, et al. 2021. Differentially private federated knowledge graphs embedding. In *CIKM*. ACM, 1416–1425.
- [34] Le Trieu Phong, Yoshinori Aono, Takuya Hayashi, Lihua Wang, and Shiro Mori. 2018. Privacy-Preserving Deep Learning via Additively Homomorphic Encryption. *IEEE Trans. Inf. Forensics Secur.* 13, 5 (2018), 1333–1345.
- [35] Joachim Scherer and Gerd Kiparski. 2018. The Eu General Data Protection Regulation (Gdpr): A Commentary. *Comput. und Recht* 34, 6 (2018), 69–70.
- [36] Divya Anand Sinha, Yezli Liu, Ruojie Du, and Yanning Shen. 2024. Gradient Inversion Attack on Graph Neural Networks. *arXiv preprint arXiv:2411.19440* (2024).
- [37] Yue Tan, Yixin Liu, Guodong Long, Jing Jiang, et al. 2023. Federated learning on non-iid graphs via structural knowledge sharing. In *AAAI*. 9953–9961.
- [38] Mark Vero, Mislav Balunovic, Dimitar Iliev Dimitrov, et al. 2023. TabLeak: Tabular Data Leakage in Federated Learning. In *ICML*. Vol. 202. PMLR, 35051–35083.
- [39] Jia Wang, Yawen Li, Zhi Xue, Yingxia Shao, Zeli Guan, and Wenling Li. 2025. Horizontal Federated Heterogeneous Graph Learning: A Multi-Scale Adaptive Solution to Data Distribution Challenges. In *WWW*. ACM, 4582–4591.
- [40] Yijue Wang, Jieren Deng, Dan Guo, Chenghong Wang, Xianrui Meng, Hang Liu, Caiwen Ding, and Sangthavar Rajasekaran. 2020. SAPAG: A Self-Adaptive Privacy Attack From Gradients. *CoRR* abs/2009.06228 (2020).
- [41] Zifan Wang, Changgen Peng, Xing He, and Weijie Tan. 2023. Wasserstein Distance-Based Deep Leakage from Gradients. *Entropy* 25, 5 (2023), 810.

- [42] Shuyue Wei, Yongxin Tong, Zimu Zhou, Yi Xu, Jingkai Gao, Tongyu Wei, Tianran He, and Weifeng Lv. 2025. Federated reasoning LLMs: a survey. *Frontiers Comput. Sci.* 19, 12 (2025), 1912613.
- [43] Shuyue Wei, Yuanyuan Zhang, Zimu Zhou, Tianlong Zhang, and Ke Xu. 2024. FedSM: A Practical Federated Shared Mobility System. *Proceedings of the VLDB Endowment* 17, 12 (2024), 4445–4448.
- [44] Wenyi Wei, Ling Liu, Margaret Loper, et al. 2020. A framework for evaluating client privacy leakages in federated learning. In *ESORICS*. Springer, 545–566.
- [45] Zonghan Wu, Shirui Pan, Fengwen Chen, Guodong Long, Chengqi Zhang, and Philip S. Yu. 2021. A Comprehensive Survey on Graph Neural Networks. *IEEE Trans. Neural Networks Learn. Syst.* 32, 1 (2021), 4–24.
- [46] Han Xie, Jing Ma, Li Xiong, et al. 2021. Federated graph classification over non-iid graphs. In *NeurIPS*.
- [47] Linghua Yang, Wantong Chen, Xiaoxi He, Shuyue Wei, Yi Xu, Zimu Zhou, and Yongxin Tong. 2024. FedGTP: Exploiting Inter-Client Spatial Dependency in Federated Graph-based Traffic Prediction. In *KDD*. ACM, 6105–6116.
- [48] Qiang Yang, Yang Liu, Tianjian Chen, and Yongxin Tong. 2019. Federated Machine Learning: Concept and Applications. *ACM Trans. Intell. Syst. Technol.* 10, 2 (2019), 12:1–12:19.
- [49] Mang Ye, Xiuwen Fang, Bo Du, Pong C. Yuen, and Dacheng Tao. 2024. Heterogeneous Federated Learning: State-of-the-art and Research Challenges. *ACM Comput. Surv.* 56, 3 (2024), 79:1–79:44.
- [50] Hongxi Yin, Arun Mallya, Arash Vahdat, Jose M Alvarez, Jan Kautz, and Pavlo Molchanov. 2021. See through gradients: Image batch recovery via gradinversion. In *CVPR*. 16337–16346.
- [51] Xuefei Yin, Yanming Zhu, and Jiankun Hu. 2022. A comprehensive survey of privacy-preserving federated learning: A taxonomy, review, and future directions. *ACM Comput. Surv.* 54, 6 (2022), 131:1–131:36.
- [52] Ke Zhang, Carl Yang, Xiaoxiao Li, Lichao Sun, et al. 2021. Subgraph federated learning with missing neighbor generation. In *NeurIPS*.
- [53] Rui Zhang, Song Guo, Junxiao Wang, et al. 2023. A Survey on Gradient Inversion: Attacks, Defenses and Future Directions. In *IJCAI*. ijcai.org, 5678–685.
- [54] Xian-Da Zhang. 2017. *Matrix analysis and applications*. Cambridge University Press.
- [55] Ziwei Zhang, Peng Cui, and Wenwu Zhu. 2022. Deep Learning on Graphs: A Survey. *IEEE Trans. Knowl. Data Eng.* 34, 1 (2022), 249–270.
- [56] Bo Zhao, Konda Reddy Mopuri, and Hakai Bilen. 2020. iDLG: Improved Deep Leakage from Gradients. *CoRR* abs/2001.02610 (2020).
- [57] Zhiqiang Zhong and Davide Mottin. 2023. Knowledge-augmented Graph Machine Learning for Drug Discovery: From Precision to Interpretability. In *KDD*. ACM, 5841–5842.
- [58] Junyi Zhu and Matthew B. Blaschko. 2021. R-GAP: Recursive Gradient Attack on Privacy. In *ICLR*.
- [59] Ligeng Zhu, Zhijian Liu, and Song Han. 2019. Deep leakage from gradients. In *NeurIPS*.

A APPENDIX

A.1 More Details for Data Leakage Analysis

Pooling as matrix operations. Common pooling methods can be represented as the following matrix operation on the node embedding matrix of the l -th layer $H_l \in \mathbb{R}^{|V| \times d_H}$. Specifically, for the sum pooling where $H_G = \sum_{v \in G} h_v$, it can be described as the sum of each row (i.e., each node) in H_l . This operation is performed using the all-ones vector $M_{p_sum}^\top = 1^{|V|} \in \mathbb{R}^{|V|}$ and $H_G = M_{p_sum} H_l$. Similarly, for mean pooling where $H_G = \frac{1}{|V|} \sum_{v \in G} h_v$, it can be calculated as $H_G = \frac{1}{|V|} M_{p_sum} H_l$. As for the max pooling, we initially approximate the maximum function by $\max(X) = \frac{1}{K} \log \sum_{i=1}^D e^{KX_i}, X \in \mathbb{R}^D$, where K is an integer. By incorporating it into max pooling where $H_G = \max_{v \in G} h_v$, the max pooling can be expressed as $H_G = \frac{1}{K} f_{\log}(M_{p_sum} f_{\exp}(K H_l))$, where $f_{\log}(\cdot)$ and $f_{\exp}(\cdot)$ represent the element-wise functions $\log(\cdot)$ and $\exp(\cdot)$, which only impacts ∇W_l in Lemma 1. Thus, we have $\nabla W_l = H_{l-1}^\top \bar{A}^\top (M_p^\top (\frac{\partial L}{\partial \bar{Y}} W_{fc} \odot F_{\log}') \odot F_{\exp}') \odot \sigma_l'$ and the recursive rule remains valid.

Discussion on deriving σ' . σ' represents the derivation of the activation function, which in GNN is typically the ReLU function. Since we calculate the node embeddings in a reverse manner, we can derive σ_{l-1}' from its output H_l . Specifically, for the ReLU function, the derivative is 1 for each positive element in H_l and 0 otherwise. In the last layer, obtaining node embeddings from the pooling result is challenging, so we initialize it as all ones. This aims to leverage as much information as possible, considering that other components in the equations, such as the adjacency matrix, are often sparse. While this may introduce some error, the experimental results in the paper demonstrate that our proposed approach achieves better performance compared with other baselines.

A.2 Proofs of Lemma 1 and Theorem 1

We first introduce two basic facts [54] that are widely used in matrix derivatives to aid the gradient computation in this work.

FACT 1. *The full differential of a function $f : \mathbb{R}^{n \times m} \rightarrow \mathbb{R}$ w.r.t. an $n \times m$ matrix X can be expressed by trace and matrix derivatives as,*

$$df(X) = \text{tr}(\frac{\partial f(X)}{\partial X}^\top dX) = \text{tr}(\frac{\partial f(X)}{\partial X} dX^\top) \quad (22)$$

Here $\frac{\partial f(X)}{\partial X}$ is the derivative matrix of f with respect to X and dX denotes the infinitesimal change in X . $\text{tr}(\cdot)$ is the trace operation.

FACT 2. *For a function $f : \mathbb{R}^{n \times m} \rightarrow \mathbb{R}$ with respect to an $n \times m$ matrix X , the following equation holds:*

$$df(X) = \text{tr}(df(X)) \quad (23)$$

Based on above two facts, we can prove the Lemma 1 in Sec. 4.1.

LEMMA 1 (GRADIENTS IN AN l -LAYER GCN). *For the GCN layers in FGL, the gradients $\nabla W_l, \nabla W_{l-1}, \nabla W_{l-2}$ can be formally expressed by the node embeddings from their previous layer $H_{l-1}, H_{l-2}, H_{l-3}$ respectively and the normalized graph adjacency matrix \bar{A} ,*

$$\nabla W_l = H_{l-1}^\top \bar{A}^\top (M_p^\top \frac{\partial L}{\partial \bar{Y}} W_{fc} \odot \sigma_l') \quad (24)$$

$$\nabla W_{l-1} = H_{l-2}^\top \bar{A}^\top (A^\top (M_p^\top \frac{\partial L}{\partial \bar{Y}} W_{fc} \odot \sigma_l') W_l^\top \odot \sigma_{l-1}') \quad (25)$$

$$\nabla W_{l-2} = H_{l-3}^\top \bar{A}^\top (A^\top (M_p^\top \frac{\partial L}{\partial \bar{Y}} W_{fc} \odot \sigma_l') W_l^\top \odot \sigma_{l-1}') W_{l-1}^\top \odot \sigma_{l-2}' \quad (26)$$

PROOF. Following Fact 2, we calculate the full differential of the loss function w.r.t W_l as $dL = \text{tr}(dL) = \text{tr}(\frac{dL}{d\bar{Y}} d\bar{Y})$. By Eq. (4)-Eq. (5), the above loss function can be further transformed as follows:

$$dL = \text{tr}(\frac{dL}{d\bar{Y}} W_{fc} d(H_l^\top) M_p^\top) = \text{tr}(M_p^\top \frac{dL}{d\bar{Y}} W_{fc} d(\sigma_l (W_l^\top H_{l-1}^\top \bar{A}^\top))) \quad (27)$$

As the activation function σ includes the element-wise Hadamard product, we can use the property of the trace of the product, $\text{tr}(A(B \odot C)) = \text{tr}((A \odot B^\top) C)$, to further derive the loss function as:

$$\begin{aligned} dL &= \text{tr}(M_p^\top \frac{dL}{d\bar{Y}} W_{fc} ((\sigma_l^\top)' \odot d(W_l^\top H_{l-1}^\top \bar{A}^\top))) \\ &= \text{tr}((M_p^\top \frac{dL}{d\bar{Y}} W_{fc} \odot \sigma_l') d(W_l^\top H_{l-1}^\top \bar{A}^\top)) = \text{tr}(H_{l-1}^\top \bar{A}^\top (M_p^\top \frac{dL}{d\bar{Y}} W_{fc} \odot \sigma_l') dW_l^\top) \end{aligned} \quad (28)$$

According to Fact 1, we have following result,

$$\nabla W_l = \frac{\partial L}{\partial W_l} = H_{l-1}^\top \bar{A}^\top (M_p^\top \frac{dL}{d\bar{Y}} W_{fc} \odot \sigma_l') \quad (29)$$

Extending H_{l-1} in the last line of Eq. (28) to the previous layer using the propagation rule of GCN, we can further calculate the full differential of the loss function with respect to W_{l-1} :

$$\begin{aligned} dL &= \text{tr}(\bar{A}^\top (M_p^\top \frac{dL}{d\bar{Y}} W_{fc} \odot \sigma_l') W_l^\top dH_{l-1}^\top) \\ &= \text{tr}(\bar{A}^\top (M_p^\top \frac{dL}{d\bar{Y}} W_{fc} \odot \sigma_l') W_l^\top d(\sigma_{l-1} (W_{l-1}^\top H_{l-2}^\top \bar{A}^\top))) \end{aligned} \quad (30)$$

Similar to Eq. (28), we can derive dW_{l-1} as follows:

$$\begin{aligned} dL &= \text{tr}(\bar{A}^\top (M_p^\top \frac{dL}{d\bar{Y}} W_{fc} \odot \sigma_l') W_l^\top ((\sigma_{l-1}^\top)' \odot d(W_{l-1}^\top H_{l-2}^\top \bar{A}^\top))) \\ &= \text{tr}((\bar{A}^\top (M_p^\top \frac{dL}{d\bar{Y}} W_{fc} \odot \sigma_l') W_l^\top \odot \sigma_{l-1}') d(W_{l-1}^\top H_{l-2}^\top \bar{A}^\top)) \\ &= \text{tr}(H_{l-2}^\top \bar{A}^\top (\bar{A}^\top (M_p^\top \frac{dL}{d\bar{Y}} W_{fc} \odot \sigma_l') W_l^\top \odot \sigma_{l-1}') dW_{l-1}^\top) \end{aligned} \quad (31)$$

Therefore, we can get the following equation based on Fact 1:

$$\nabla W_{l-1} = \frac{\partial L}{\partial W_{l-1}} = H_{l-2}^\top \bar{A}^\top (\bar{A}^\top (M_p^\top \frac{dL}{d\bar{Y}} W_{fc} \odot \sigma_l') W_l^\top \odot \sigma_{l-1}') \quad (32)$$

Similarly, gradients for W_{l-2} can be obtained by extending H_{l-2} ,

$$\begin{aligned} dL &= \text{tr}(\bar{A}^\top (\bar{A}^\top (M_p^\top \frac{dL}{d\bar{Y}} W_{fc} \odot \sigma_l') W_l^\top \odot \sigma_{l-1}') W_{l-1}^\top dH_{l-2}^\top) \\ &= \text{tr}(\mathbf{r}_{l-1} W_{l-1}^\top dH_{l-2}^\top) = \text{tr}(\mathbf{r}_{l-1} W_{l-1}^\top d(\sigma_{l-2} (W_{l-2}^\top H_{l-3}^\top \bar{A}^\top))) \end{aligned} \quad (33)$$

where \mathbf{r}_{l-1} is defined as $\bar{A}^\top (\bar{A}^\top (M_p^\top \frac{dL}{d\bar{Y}} W_{fc} \odot \sigma_l') W_l^\top \odot \sigma_{l-1}')$ to enhance the clarity of the equation. Once again, leveraging the noted property of the Hadamard operation, we derive dW_{l-2} as follows:

$$\begin{aligned} dL &= \text{tr}(\mathbf{r}_{l-1} W_{l-1}^\top ((\sigma_{l-2}^\top)' \odot d(W_{l-2}^\top H_{l-3}^\top \bar{A}^\top))) \\ &= \text{tr}((\mathbf{r}_{l-1} W_{l-1}^\top \odot \sigma_{l-2}') d(W_{l-2}^\top H_{l-3}^\top \bar{A}^\top)) = \text{tr}(H_{l-3}^\top \bar{A}^\top (\mathbf{r}_{l-1} W_{l-1}^\top \odot \sigma_{l-2}') dW_{l-2}^\top). \end{aligned} \quad (34)$$

Then, we obtain the gradients ∇W_{l-2} ,

$$\nabla W_{l-2} = \frac{\partial L}{\partial W_{l-2}} = H_{l-3}^\top \bar{A}^\top (\bar{A}^\top (M_p^\top \frac{dL}{d\bar{Y}} W_{fc} \odot \sigma_l') W_l^\top \odot \sigma_{l-1}') W_{l-1}^\top \odot \sigma_{l-2}'. \quad \square$$

Next, we prove the Theorem 1 in Sec. 4.1, focusing on extending the recursive rule observed in Lemma 1 to any layer of GCNs.

Table 5: Visualization of the reconstruction performance for GraphDLG and baselines. The first graph for each row represents the ground truth. In each graph, nodes of different colors indicate different node types.

Node Feature	MSE/ACC(%)	Random	DLG	iDLG	InverGrad	GI-GAN	GRA-GRF	TableLeak	Graph-Attacker	GraphDLG (ours)
Adjacency Matrix	AUC/AP	0.3441/20.00 0.4444/0.7336	1.0625/40.00 0.8730/0.9135	0.5000/60.00 0.6984/0.8822	0.3879/60.00 0.8254/0.9115	0.2680/20.00 0.4444/0.6984	0.2209/60.00 0.3651/0.6735	0.4717/40.00 0.8254/0.9041	0.9629/40.00 0.7897/0.8706	0.0988/100.00 1.0000/1.0000
Ground-truth/ Reconstructed graph										
Node Feature	MSE/ACC(%)	0.3836/33.33 0.4514/0.6142	2.4573/33.33 0.4444/0.7148	2.1012/50.00 0.7604/0.8430	1.4808/50.00 0.6354/0.6981/63.89	0.2096/66.67 0.4583/0.6488	0.1744/50.00 0.5000/0.6667	0.5025/16.67 0.8264/0.9009	1.7374/0.00 0.6250/0.7302	0.2007/66.67 0.9306/0.9677
Ground-truth/ Reconstructed graph										
Node Feature	MSE/ACC(%)	0.3224/26.32 0.4494/0.1083	0.9537/21.05 0.5209/0.1221	1.2781/15.79 0.5515/0.1661	0.7949/31.58 0.5357/0.1504	0.0994/57.89 0.5110/0.1243	0.1072/ 84.21 0.4209/0.1101/49.86	0.3175/26.32 0.5528/0.1396	0.8379/21.05 0.5119/0.1245	0.0745/84.21 0.9865/0.9203
Ground-truth/ Reconstructed graph										
Node Feature	MSE/ACC(%)	0.3282/0.00 0.5070/0.0736	1.0487/3.33 0.4598/0.0641	0.9469/16.67 0.5070/0.0695	0.9277/13.33 0.4840/0.0682	0.0274/0.00 0.5470/0.0780	0.0154/ 80.00 0.4796/0.0686	0.3174/6.67 0.4445/0.0662	1.0269/10.00 0.5319/0.0756	0.0144/80.00 0.9238/0.4942
Ground-truth/ Reconstructed graph										
Node Feature	MSE/ACC(%)	0.3218/4.35 0.4541/0.0425	0.9578/13.04 0.4241/0.0407	1.0178/10.87 0.4967/0.0471	0.9178/4.35 0.4780/0.0448	0.0274/0.00 0.4638/0.0452	0.0193/69.57 0.4790/0.0464	0.3077/2.17 0.5886/0.0644	1.0710/6.52 0.5053/0.0487	0.3580/71.74 0.8740/0.2678
Ground-truth/ Reconstructed graph										

THEOREM 1 (RECURSIVE RULE FOR GRADIENTS). *The gradients ∇W_i in GCN can be depicted by its input embedding H_{i-1} and a coefficient matrix \mathbf{r}_i in a closed-form recursive equation, i.e., $\nabla W_i = H_{i-1}^\top \mathbf{r}_i$, where the coefficient matrix \mathbf{r}_i is defined as follows,*

$$\mathbf{r}_i = \begin{cases} \bar{A}^\top (M_p^\top \frac{\partial L}{\partial Y} W_{fc} \odot \sigma'_i), & i = l \\ \bar{A}^\top (r_{i+1} W_{i+1}^\top \odot \sigma'_i), & i = 1, \dots, l-1 \end{cases} \quad (35)$$

PROOF. When $i = l$, it can be proved by rewriting Eq. (24) in Lemma 1 as $\nabla W_l = H_{l-1}^\top \mathbf{r}_l$, where $\mathbf{r}_l = \bar{A}^\top (M_p^\top \frac{\partial L}{\partial Y} W_{fc} \odot \sigma'_l)$.

When $i = l-1, l-2, \dots, 1$, we will utilize mathematical induction to prove the equation $dL = \text{tr}(\mathbf{r}_i W_i^\top dH_{i-1}^\top)$, $i = 1, \dots, l-1$. Then, we can also establish the proof of Theorem 1 by induction. Our proof consists of two steps: the base case and the induction step.

Step 1: Base Case. When $i = l-1$, we have $r_{l-1} = \bar{A}^\top (r_l W_l^\top \odot \sigma'_l) = \bar{A}^\top (\bar{A}^\top (M_p^\top \frac{\partial L}{\partial Y} W_{fc} \odot \sigma'_l) W_l^\top \odot \sigma'_{l-1})$. By Eq. (25) and Eq. (33), $\nabla W_{l-1} = H_{l-2}^\top \mathbf{r}_{l-1}$ and $dL = \text{tr}(\mathbf{r}_{l-1} W_{l-1}^\top dH_{l-2}^\top)$ are true.

Step 2: Induction Step. Next, we assume that the formulas are true for any arbitrary positive integer k ($1 < k \leq l-1$). We aim to prove that when $i = k-1$, $dL = \text{tr}(\mathbf{r}_i W_i^\top dH_{i-1}^\top)$ also hold true.

According to the induction hypothesis, we have:

$$dL = \text{tr}(\mathbf{r}_k W_k^\top dH_{k-1}^\top) = \text{tr}(\mathbf{r}_k W_k^\top d(\sigma_{k-1} (W_{k-1}^\top H_{k-2}^\top \bar{A}^\top))) \quad (36)$$

By the property of Hadamard operation in Eq. (34), we have,

$$\begin{aligned} dL &= \text{tr}(\mathbf{r}_k W_k^\top ((\sigma_{k-1}^\top) \odot d(W_{k-1}^\top H_{k-2}^\top \bar{A}^\top))) = \text{tr}((\mathbf{r}_k W_k^\top \odot \sigma'_{k-1}) d(W_{k-1}^\top H_{k-2}^\top \bar{A}^\top)) \\ &= \text{tr}(H_{k-2}^\top \bar{A}^\top (\mathbf{r}_k W_k^\top \odot \sigma'_{k-1}) dW_{k-1}^\top) = \text{tr}(H_{k-2}^\top \mathbf{r}_{k-1} dW_{k-1}^\top) \end{aligned} \quad (37)$$

where \mathbf{r}_{k-1} is as its definition, i.e., $\mathbf{r}_{k-1} = \bar{A}^\top (\mathbf{r}_k W_k^\top \odot \sigma'_{k-1})$.

Thus, we have $\nabla W_{k-1} = \frac{\partial L}{\partial W_{k-1}} = H_{k-2}^\top \mathbf{r}_{k-1}$. Then, we can compute the full differential w.r.t. H_{k-2} based on Eq. (37):

$$dL = \text{tr}((\mathbf{r}_k W_k^\top \odot \sigma'_{k-1}) W_k^\top dH_{k-2}^\top \bar{A}^\top) = \text{tr}(\mathbf{r}_{k-1} W_{k-1}^\top dH_{k-2}^\top) \quad (38)$$

As previous assumptions also hold, we establish the induction step.

Conclusion. Finally, by mathematical induction, we finish the proof. \square

A.3 More Implementation Details

Experimental Environment. We implement all methods using PyTorch 2.2.1 and the PyTorch Geometric (PyG) library. All experiments were conducted on an NVIDIA A100-PCIE-40GB server with CUDA 11.8 and Intel(R) Xeon(R) Gold 6230R CPU @ 2.10GHz. We utilize the PyG library to handle the mentioned graph datasets, which involves removing isomorphic graphs. During partitioning, we divide the datasets into two parts based on the graph labels employing Dirichlet distribution with $\alpha = 1.0$, widely used for simulating a non-i.i.d (heterogeneous) setting in federated learning.

A.4 Baseline Descriptions

The main ideas of the baselines is presented as follows.

- Random:** It randomly generates both graph structures and features from a uniform distribution.
- DLG** [59]: It is the seminar work that introduces an optimization process based on gradient matching using L2 distance and the L-BFGS optimizer. For extension to graphs, we initialize both the adjacency matrix and node features as dummy data.
- iDLG** [56]: It improves DLG by introducing label inference from gradients to enhance recovery.
- InverGrad** [13]: It employs an optimization framework with cosine distance and the Adam optimizer, along with a total variation loss originally tailored for images. As its total variation loss is unsuitable for graphs, we omit it in our implementation.
- GI-GAN**: It represents the GAN-based approaches [18, 25] that optimize a dummy latent vector and feed it into a pre-trained GAN for recovery, thereby leveraging GAN-learned priors. Specifically, we adopt MolGAN [1] as an extension for graph data.

Table 7: Performance with deeper GCN models.

Method	3-layer-GCN						4-layer-GCN					
	Node Feature			Graph Structure			Node Feature			Graph Structure		
	MSE	ACC (%)	AUC	AP	ACC (%)	AUC	MSE	ACC (%)	AUC	AP	ACC (%)	
Random	0.3430	11.99	0.4896	0.1325	49.51		0.3416	13.29	0.4996	0.1382	49.89	
DLG	1.1412	21.45	0.5344	0.1423	65.06		1.2389	19.62	0.5269	0.1412	64.89	
iDLG	1.1519	16.76	0.5371	0.1481	65.67		1.2162	18.28	0.5176	0.1386	64.62	
InverGrad	1.0014	22.96	0.5397	0.1490	56.62		1.0559	22.51	0.5102	0.1396	58.43	
GI-GAN	1.1054	51.89	0.5091	0.1248	14.03		0.1054	51.99	0.5092	0.1248	14.06	
GRA-GRF	0.1079	71.06	0.4831	0.1231	49.19		0.1080	73.31	0.4922	0.1237	50.36	
GraphDLC	0.0683	74.34	0.9032	0.7562	93.41	0.0848	74.33	0.9022	0.7556	93.41		

- **GRA-GFA** [2]: It extends DLG to reconstruct graph data from optimized node embeddings H . Specifically, it recovers the adjacency matrix as $\sigma(HH^T)$ and reconstructs node features using a generator that takes the inferred adjacency matrix and a randomly initialized feature matrix as input.
- **TabLeak** [38]: It is originally designed for tabular data. We extend it for graph data by treating adjacency matrices as continuous features and node attributes as discrete features, while employing its entropy-based uncertainty quantification to assess reconstruction quality.
- **Graph Attacker** [36]: it reconstructs graph data by matching dummy gradients with actual gradients while enforcing graph-specific properties through feature smoothness and sparsity regularization terms in the optimization objective.

A.5 More Case Study Results

Tab. 5 shows visualization results for various concrete biometric or chemical molecules in the performance comparison experiment, including the reconstruction results for GraphDLC and baselines. We can draw a similar conclusion to that mentioned in Sec. 5.2: Our method outperforms in recovering both the atom (node) type and the molecule structure, while other baselines tend to reconstruct a fully connected graph and incorrect node types, especially as the number of nodes increases, failing to recover the atom types and molecule structure. However, it remains challenging to reconstruct graphs with complex structures and a large number of nodes.

A.6 More Experimental Studies

Studies on Larger Batch Sizes. We further compare the proposed method with baselines under larger batch sizes to validate the effectiveness. As shown in Tab. 6 on the MUTAG dataset, GraphDLC consistently outperforms the baselines across different batch sizes, achieving an oblivious improvement of 16.35% in node feature ACC and 66.58% in graph structure AUC, thereby demonstrating the effectiveness and robustness of our approach.

Table 6: Performance with larger batch sizes.

Method	Batch size=4			Batch size=8			Batch size=16		
	Feature			Structure			Feature		
	ACC (%)	AUC	AP	ACC (%)	AUC	AP	ACC (%)	AUC	AP
Random	13.82	0.4917	0.1423	13.70	0.5009	0.1357	14.57	0.5054	0.1390
DLG	14.95	0.5208	0.1465	18.06	0.5149	0.1410	14.33	0.5243	0.1440
iDLG	17.20	0.5339	0.1498	15.13	0.5394	0.1466	14.70	0.5427	0.1476
InverGrad	23.10	0.5428	0.1532	21.66	0.5367	0.1504	22.03	0.5379	0.1488
GI-GAN	45.52	0.5059	0.1240	38.11	0.5046	0.1237	44.88	0.5085	0.1251
GRA-GRF	19.50	0.4893	0.1230	20.89	0.4970	0.1250	17.60	0.4852	0.1220
GraphDLC	61.87	0.9042	0.7554	68.08	0.9043	0.7558	65.10	0.9042	0.7557

Studies on Deeper GCN Model. Tab. 7 reports results using deeper GCN models with 3 and 4 layers on MUTAG dataset. The results show that the proposed GraphDLC consistently outperforms other

baselines in both feature and structure recovery, reducing the MSE of node features by over 19.54% and improving the AUC of graph structures by more than 67.35%, *i.e.* our approach still achieves the best recovery performance for graph-tailored DLG.

Studies on Larger Hidden Size. Tab. 8 shows the results using larger hidden sizes on MUTAG dataset. We further conducted experiments with larger hidden sizes of 64 and 128, respectively. The results are as follows. It is evident that our proposed GraphDLC maintains the best feature and structure recovery performance compared with all baselines, reducing node features' MSE by over 8.07% and increasing graph structure's AUC by over 64.57%.

Table 8: Performance comparison using larger hidden sizes.

Method	Hidden size = 64						Hidden size = 128					
	Node Feature			Graph Structure			Node Feature			Graph Structure		
	MSE	ACC (%)	AUC	AP	ACC (%)	AUC	MSE	ACC (%)	AUC	AP	ACC (%)	
Random	0.3316	14.77	0.4789	0.1344	49.18		0.3337	15.05	0.4912	0.1331	49.67	
DLG	1.1304	20.46	0.5283	0.1469	65.88		1.0489	21.48	0.5236	0.1444	62.88	
iDLG	1.1228	20.29	0.5425	0.1577	65.57		1.1215	19.47	0.5265	0.1471	64.97	
InverGrad	0.9400	25.09	0.5492	0.1615	54.70		0.8657	25.41	0.5380	0.1561	49.11	
GI-GAN	0.1053	50.33	0.5108	0.1254	14.85		0.1050	52.37	0.5020	0.1234	14.42	
GRA-GRF	0.1078	71.78	0.4813	0.1210	52.19		0.1077	71.72	0.4831	0.1216	53.38	
GraphDLC	0.0968	73.88	0.9038	0.7560	93.41	0.0870	74.34	0.9041	0.7557			

A.7 Potential Defense Methods

We further conducted experiments to study the potential defense strategies against the proposed attack. *DP-Gradients*: it follows the classical differential privacy mechanism by adding Laplacian noise with variance σ to model gradients *(ii) DP-Activations*: it injects Laplacian noise with variance σ into the activations (*i.e.*, layer outputs) of GCN layers instead of the gradients. *(iii) DP-Hybrid*: it is a combined scheme that applies Laplacian noise with variance $\sigma/2$ to both gradients and activations, respectively. The experimental results summarized in Tab. 9, where we highlight the best result in bold and the second best result with the symbol “*”.

Experimental Observations. Firstly, the DP-Gradients provides stronger protection for node features than for graph structures, which is consistent with the results shown in Fig. 4. Nevertheless, when σ is large (*e.g.*, $\sigma = 0.5$), it can also offer meaningful protection for the graph structure. Secondly, the DP-Activations is more effective in protecting graph structure, likely because the graph structure plays a central role in graph convolution operations, where injecting noise into intermediate activations directly disrupts the structure-related signals. Finally, the DP-Hybrid appear to be a promising defense strategy, as it combines the advantages of both DP-Gradients and DP-Activations, *i.e.*, the DP-Hybrid can provide comprehensive protection for both node features and graph structures. *In summary, injecting noise into both gradients and activations simultaneously can serve as an effective defense strategy against deep leakage from gradients in federated graph learning.*

Table 9: Results on Three Potential Defense Methods with Varying Noise Levels (σ).

Defense	DP-Gradients			DP-Activations			DP-Hybrid		
	Feature			Structure			Feature		
	ACC (%)	AUC	AP	ACC (%)	AUC	AP	ACC (%)	AUC	AP
w/o DP	74.35	0.9042	0.7556	74.35	0.9042	0.7556	74.35	0.9042	0.7556
$\sigma=0.05$	63.50	0.9045	0.7564	74.34	0.8994*	0.7358*	67.99*	0.8843	0.7079
$\sigma=0.1$	36.50	0.8931	0.7296	74.34	0.8820*	0.6926*	45.49*	0.8546	0.6618
$\sigma=0.2$	25.22	0.8820	0.7204	74.34	0.8485*	0.6351*	29.26*	0.8328	0.6313
$\sigma=0.5$	20.67	0.8272*	0.6230*	74.34	0.8131	0.5748	20.75*	0.8344	0.6404